HIGD-1B inhibits hypoxia-induced mitochondrial fragmentation by regulating OPA1 cleavage in cardiomyocytes

YAN PANG[1], ZHIDE ZHU[2], ZHIHAO WEN[1], JUNSHEN LU[3], HAO LIN[4], MEILING TANG[1], ZHILIANG XU[2] and JIANQI LU[1]

[1]Department of Cardiology, The First Affiliated Hospital, Guangxi University of Chinese Medicine, Nanning, Guangxi 530023; [2]Academic Affairs Section, Guangxi University of Chinese Medicine, Nanning, Guangxi 530000; [3]Academic Affairs Section, Guangxi University of Traditional Chinese Medicine Attached Chinese Medicine School, Nanning, Guangxi 530001; [4]Department of Geriatrics, Danzhou Traditional Chinese Medicine Hospital, Danzhou, Hainan 571700, P.R. China

Received August 17, 2020; Accepted March 9, 2021

DOI: 10.3892/mmr.2021.12188

Abstract. The dynamic regulation of mitochondrial morphology is key for eukaryotic cells to manage physiological challenges. Therefore, it is important to understand the molecular basis of mitochondrial dynamic regulation. The aim of the present study was to explore the role of HIG1 hypoxia inducible domain family member 1B (HIGD-1B) in hypoxia-induced mitochondrial fragmentation. Protein expression was determined via western blotting. Immunofluorescence assays were performed to detect the subcellular location of HIGD-1B. Cell Counting Kit-8 assays and flow cytometry were carried out to measure cell viability and apoptosis, respectively. Protein interactions were evaluated by co-immunoprecipitation. In the present study, it was found that HIGD-1B serves a role in cell survival by maintaining the integrity of the mitochondria under hypoxic conditions. Knockdown of HIGD-1B promoted mitochondrial fragmentation, while overexpression of HIGD-1B increased survival by preventing activation of caspase-3 and -9. HIGD-1B expression was associated with cell viability and apoptosis in cardiomyocytes. Furthermore, HIGD-1B delayed the cleavage process of optic atrophy 1 (OPA1) and stabilized mitochondrial morphology by interacting with OPA1. Collectively, the results from the present study identified a role for HIGD-1B as an inhibitor of the mitochondrial fission in cardiomyocytes.

Correspondence to: Professor Jianqi Lu, Department of Cardiology, The First Affiliated Hospital, Guangxi University of Chinese Medicine, 89-9 Dongge Road, Qingxiu, Nanning, Guangxi 530023, P.R. China
E-mail: jianqilu1245@hotmail.com

Key words: HIG1 hypoxia inducible domain family member 1B, optic atrophy 1, hypoxia, mitochondria, cardiomyocyte

Introduction

Mitochondria are essential subcellular organelles that are involved in respiration, oxidative phosphorylation and apoptosis. Balanced cycles of fusion and fission are essential for maintaining mitochondrial morphology and activity (1). An aberrant balance between fission and fusion is associated with a number of neurodegenerative disorders and cardiac diseases (2,3). For example, peroxisome proliferator-activated receptor-γ coactivator-1α (PGC-1α) expression, which is decreased in postmortem brains of patients with Parkinson's disease, protected against neurotoxicity induced by 1-methyl-4-phenyl-1,2,3,6-tetrahydrodropyridine (4). Fission is regulated by dynamin-related protein 1 (DRP1), which can assemble into multimeric ring-like structures and wrap around the constriction sites of dividing mitochondria (5). Mitochondrial outer membrane dynamin-like guanosine triphosphatases (GTPases) mitofusin (MFN)-1 and -2 orchestrate outer mitochondrial membrane fusion (6), while optic atrophy 1 (OPA1) is required for inner mitochondrial membrane fusion (7). OPA1 is encoded by eight mRNA splice forms, which are produced by differential splicing. Cleavage of OPA1 is a key regulatory step for coordinating fusion and fission of mitochondria (8). There are two mitochondrial inner membrane-embedded AAA proteases (*i*-AAA), metalloendopeptidase OMA1, mitochondrial (OMA1) and ATP-dependent zinc metalloprotease YME1L1 (YME1L), which can convert long forms (L-OPA1) into short forms (S-OPA1). The *i*-AAA protease YME1L regulates OPA1 cleavage at site S2, whereas OMA1 mediates mitochondrial fragmentation by transformation of L-OPA1 into S-OPA1 at site S1 (9,10). The balance between the two forms of OPA1 maintains normal mitochondrial morphology; fusion involves L-OPA1, whereas S-OPA1 is associated with fission (11,12). Furthermore, OPA1 serves an important role in maintaining mitochondrial inner structure and crista remodeling (13).

Hypoxia is associated with heart disease, stroke and tumor microenvironment (14). It has also been demonstrated that hypoxia induces mitochondrial fragmentation (15). The HIG1 hypoxia inducible domain (*HIGD*) family of genes,

whose expression is induced during hypoxia, is conserved throughout evolution (16). There are five human *HIGD* genes, *HIGD-1A*, *-1B*, *-1C*, *-2A* and *-2B*. *HIGD-1A* is regulated by hypoxia-inducible factor-1 (HIF1) under hypoxic conditions. *HIGD-1A* is a survival factor that contains two transmembrane domains oriented in a 'N-terminal outside-C-terminal outside and loop inside' conformation (17). As a mitochondrial inner membrane protein, *HIGD-1A* knockdown decreases cytochrome *c* oxidase activity, leading to increased mitochondrial fission and cell death in response to hypoxia (18). Ameri *et al* (19) reported that *HIGD-1A* promotes tumor cell survival by regulating AMPK activity and levels of cellular reactive oxygen species (ROS) *in vivo*. In addition, *HIGD-1A* prevents OPA1 cleavage and is required for the functional integrity of mitochondria (20). Both *HIGD-1A* and *HIGD-2A* promote cell survival in a number of cell lines in response to hypoxia, suggesting that the *HIGD* gene family may be a potential anti-apoptosis factor (21). *HIGD-1B* and *HIGD-1A* share 42.4% homology and their similarity is highest in the transmembrane domain. However, the role of *HIGD-1B* in hypoxia-induced mitochondrial fragmentation and cell apoptosis is not clearly understood. In the present study, the biological function of *HIGD-1B* in cardiomyocytes was characterized and the underlying mechanisms were investigated. Knockdown or overexpression experiments were performed to examine the effects of HIGD-1B on OPA1 expression. The interaction between HIGD-1B and OPA1 was measured via co-immunoprecipitation (Co-IP) assays. The effect of HIGD-1B on cell viability was determined via Cell Counting Kit-8 (CCK-8) and apoptosis assays.

Materials and methods

Cell culture. AC16 human cardiomyocyte and 293T embryonic kidney cell lines were purchased from American Type Culture Collection and cultured in DMEM supplemented with 10% fetal bovine serum (both Gibco; Thermo Fisher Scientific, Inc.) and 1% penicillin-streptomycin at 37˚C in a humidified incubator with 5% CO_2. Hypoxia experiments were performed using a hypoxia chamber (Billups-Rothenberg, Inc.). AC16 cells were cultured under hypoxic conditions of 1% oxygen (5% CO_2 and 94% N_2). Small interfering (si)RNA-mediated knockdown of *HIGD-1B* was performed using specific siRNAs targeting *HIGD-1B* (cat. no. SR324184; OriGene Technologies, Inc.) and scrambled siRNAs (cat. no. SR30004; OriGene Technologies, Inc.) as a negative control.

Plasmid constructs. For the pB513B-HIGD-1B-Flag constructs, the coding sequence of *HIGD-1B* (GenBank accession no. NM_016438) was inserted into the pB513B-Flag (cat. no. 5619; BioVector NTCC, Inc.) expression vector. The coding sequence of OPA1 (GenBank accession no. NM_015560) was inserted into the pB513B-myc expression vector to generate the pB513B-OPA1-myc vector. The coding sequence of *HIGD-1B* was inserted into the pGEX-4T-1 vector to generate the pGEX-HIGD-1B-GST vector.

In vitro cell viability assay. Cell viability was determined using a CCK-8 assay (Beijing Solarbio Science & Technology Co., Ltd.), which was performed according to the manufacturer's instructions in 96-well plates. Briefly, AC16 cells were seeded ($5x10^3$ cells/well) in a 96-well plate and cultured at 37˚C for 48 h. Cells were incubated with the CCK-8 reagent for 1 h. Relative viability of cells was assessed at 450 nm absorbance. For crystal violet (CV) staining assay, cells were fixed with 4% formaldehyde at room temperature for 15 min, followed by staining with a crystal violet solution (crystal violet 0.2%, ethanol 2%) at room temperature for 10 min, and then the colonies were photographed using a dissection microscope. For trypan blue exclusion assay, 0.1 ml trypan blue stock solution (cat. no. 15250061; Thermo Fisher Scientific, Inc.) was added to 1 ml cells at room temperature for 5 min, and then the numbers of blue stained-cells and the number of total cells were counted under a light microscope at x10 magnification.

Immunofluorescence. AC16 cells were divided into the following four groups: i) control + normoxia group, cells were cultured under normoxic conditions without any treatment; ii) control + hypoxia group, cells were cultured under hypoxic conditions without any treatment; iii) Vector + hypoxia group, cells were cultured under hypoxic conditions and transfected with empty vector; and iv) HIGD-1B-Flag + hypoxia group, cells were cultured under hypoxic conditions and transfected with HIGD-1B-Flag vector. Subsequently, AC16 cells ($5x10^3$) were cultured on glass coverslips at 37˚C for 48 h, and stained with 100 nM MitoTracker red CMXRos at 37˚C for 30 min, then fixed with 4% formaldehyde at 4˚C for 30 min. After washing twice with ice-cold PBS, the samples were blocked with 1% BSA in PBS with Tween-20 (0.05%) at 4˚C for 1 h. Then, the cells were incubated overnight at 4˚C with anti-HIGD-1B antibody (1:500; cat. no. ab238867; Abcam). Next, the samples were washed with PBS and incubated at room temperature for 1 h with goat anti-rabbit IgG H&L (1:1,000; cat. no. ab96899; DyLight 488; Abcam). In order to determine the morphology of the mitochondria, the cells were classified into three types under a fluorescence microscope (magnification, x400): Tubular, intermediate and fragmented. 'Tubular' referred to the cells that exhibited the most interconnected mitochondria, while 'fragmented' referred to cells that primarily contained spherical mitochondrial segments.

Western blot analysis. Total protein was extracted from cells using RIPA buffer (Beijing Solarbio Science & Technology Co., Ltd.) in the presence of protease inhibitor cocktail and protein phosphatase inhibitor (both Thermo Fisher Scientific, Inc.). Protein concentration was quantified using a BCA kit (Takara Bio, Inc.). The proteins (30 μg) were separated via SDS-PAGE on 8% gel, and then electroblotted onto a PVDF membrane. Following blocking with 5% blocking reagent (cat. no. SW3015; Beijing Solarbio Science & Technology Co., Ltd.) at room temperature for 1 h, the membranes were incubated with the primary antibodies in 5% BSA overnight at 4˚C. Subsequently, the membranes were incubated with secondary antibodies at room temperature for 1 h. Proteins were visualized using ECL reagent (cat. no. WBKLS0050; EMD Millipore). The blots were detected using ImageLab software (version 3.0; Bio-Rad Laboratories, Inc.).

Reagents and antibodies. The following primary antibodies were used: HIGD-1B (1:2,000; cat. no. ab238867; Abcam), Bcl-2

(1:2,000; cat. no. sc-7382; Santa Cruz Biotechnology, Inc.), Bax (1:2,000; cat. no. 5023S; Cell Signaling Technology, Inc.), tubulin (1:5,000; cat. no. 2146S; Cell Signaling Technology, Inc.), heat shock protein 60 (1:3,000; cat. no. 12165S; Cell Signaling Technology, Inc.), translocase of outer mitochondrial membrane (Tomm)20 (1:2,000; cat. no. ab186735; Abcam), proliferating cell nuclear antigen (1:2,500; cat. no. ab29; Abcam), YME1L (1:1,000; cat. no. ab234744; Abcam), OMA1 (1:3,000; cat. no. ab154949; Abcam), MFN1 (1:2,000; cat. no. ab221661; Abcam), MFN2 (1:2,500; cat. no. ab205236; Abcam), OPA1 (1:1,000; cat. no. 67589S; Cell Signaling Technology, Inc.), DRP1 (1:2,000; cat. no. ab184247; Abcam), phosphorylated (p)-DRP1 (1:2,000; cat. no. ab193216; Abcam), Flag-tag (1:3,000; cat. no. 14793S; Cell Signaling Technology, Inc.), Myc-tag (1:3,000; cat. no. 2276S; Cell Signaling Technology, Inc.) and glutathione S-transferase (GST)-tag (1:3,000; cat. no. ab138491; Abcam). Secondary antibodies included HRP-conjugated anti-rabbit IgG (1:5,000; cat. no. 7074P2; Cell Signaling Technology, Inc.) and HRP-conjugated anti-mouse IgG (1:5,000; cat. no. 7076P2; Cell Signaling Technology, Inc.). Caspase-3 and -9 activity was measured with Fluorescent Assay kits (cat. nos. C1168S and C1157; Beyotime Institute of Biotechnology). Carbonyl cyanide m-chlorophenyl hydrazone (CCCP; cat. no. C2759) was purchased from Sigma-Aldrich (Merck KGaA). For CCCP treatment, 10-50 μM CCCP was added to the culture medium at 37˚C for 0, 10, 15 or 30 min before harvesting. Analysis of mitochondrial membrane potential was performed using a mitochondrial membrane potential assay kit (cat. no. 13296S; Cell Signaling Technologies, Inc.) according to the manufacturer's instructions.

Flow cytometry for apoptosis assay. For apoptosis analysis, AC16 cells were harvested and incubated with Annexin V (5 μl) and PI dye (5 μl) for 30 min in the dark using an Annexin V-FITC Apoptosis Detection kit (Beijing Solarbio Science & Technology Co., Ltd.) according to the manufacturer's instructions. The stained cells were analyzed using a flow cytometer (FACSCanto II; BD Bioscience). Data was analyzed using FlowJo version 10 (FlowJo, LLC).

Transfection and immunoprecipitation (IP). Transfection experiments were performed using Effectene Transfection Reagent (Qiagen China Co., Ltd.) according to the manufacturer's instructions. For knockdown or overexpression experiments, AC16 cells ($2x10^4$) were transfected with 20 nM siRNA-ctrl (5'-GACUAC UGGUCGUUGAACU-3'), 20 nM siRNA-HIGD-1B (5'-UAC GAAAUGUGUUAAAUCCUACUUG-3'), 1 μg empty vector or 1 μg pB513B-HIGD-1B-Flag vector at room temperature for 48 h. Cells were collected 48 h after transfection. For Co-IP experiments, 293T cells ($2x10^6$) were transfected with the aforementioned plasmids. After 24 h, cells were harvested and lysed in IP lysis buffer (Thermo Fisher Scientific, Inc.). The supernatant (1 ml) was incubated overnight at 4˚C with HIGD-1B antibody or anti-Flag M2 affinity gel (Sigma-Aldrich; Merck KGaA). The protein A/G-sepharose (100 μl) was added to the samples for 4 h. Following centrifugation (600 x g) at 4˚C for 10 min, the pellets were washed three times with 1 ml lysis buffer before resuspension in 2X Laemmli SDS-PAGE buffer, and then western blot analysis was performed according to standard western blotting procedures as described above.

In vitro pull-down assay. Recombinant GST-fused HIGD-1B protein was expressed and purified from *Escherichia coli* BL21 (DE3). The purification of OPA1-Myc was performed using a EZview red anti-c-Myc affinity gel (Sigma-Aldrich; Merck KGaA) according to the manufacturer's instructions. GST pull-down assays were performed by incubating HIGD-1B-GST, immobilized on glutathione-sepharose resin (BD Biosciences) with OPA1-Myc at 4˚C for 3 h. The beads were washed three times to remove unbound protein, and the bound proteins were eluted, separated using SDS-PAGE and detected using western blot analysis according to standard western blotting procedures as described above.

Subcellular fractionation analysis. Subcellular fractionation was performed using a Subcellular Protein Fractionation kit for Cultured Cells (Thermo Fisher Scientific, Inc.) according to the manufacturer's instructions. Briefly, cells were harvested in cytoplasmic extraction buffer at 4˚C for 10 min. Cell suspension was centrifuged 500 x g at 4˚C for 5 min, and the supernatant was transferred to a clean pre-chilled tube on ice. Membrane extraction buffer was added to the pellet at 4˚C for 10 min to isolate the membrane extract, followed by addition of nuclear extraction buffer at 4˚C for 30 min to isolate the chromatin-bound nuclear extract. Fraction purity was assessed via western blotting using antibodies against tubulin, PCNA and Tomm20, as aforementioned. The subcellular localization of HIGD-1B was predicted using the UniProt Knowledge Database (UniProt, http://www.uniprot.org).

Mitochondrial membrane potential measurement. Tetramethylrhodamine methyl ester (TMRE) fluorescence mitochondrial membrane potential was measured using a TMRM Assay Kit (cat. no. M20036; Thermo Fisher Scientific, Inc.). After transfection, AC16 cells ($1x10^5$) were incubated with 100 nM TMRE for 30 min in the dark, and then cells were visualized with a fluorescence microscope (magnification, x200).

Statistical analysis. The data are presented as the mean ± SEM (n≥3). Statistical significance was analyzed using SPSS software v22.0 (IBM Corp.). Comparison between two groups was performed using an unpaired Student's t-test, while ANOVA followed by Tukey's post hoc test was used to analyze data in >two groups. $P<0.05$ was considered to indicate a statistically significant difference.

Results

Knockdown of HIGD-1B induces mitochondrial fragmentation. In order to identify the role of HIGD-1B, it was investigated whether *HIGD-1B* was induced by hypoxia. *HIGD-1B* protein expression levels increased gradually from 0 to 12 h in AC16 cells under hypoxic conditions (Fig. 1A). According to the UniProt analysis, HIGD-1B was predicted to be a mitochondrial protein; thus, the subcellular localization of HIGD-1B was investigated in AC16 cells. HIGD-1B co-localized with MitoTracker-stained mitochondria (Fig. 1B). Consistently, subcellular fractionation analysis showed the presence of HIGD-1B in the mitochondria (Fig. 1C). Next, the morphology of mitochondria was assessed by staining

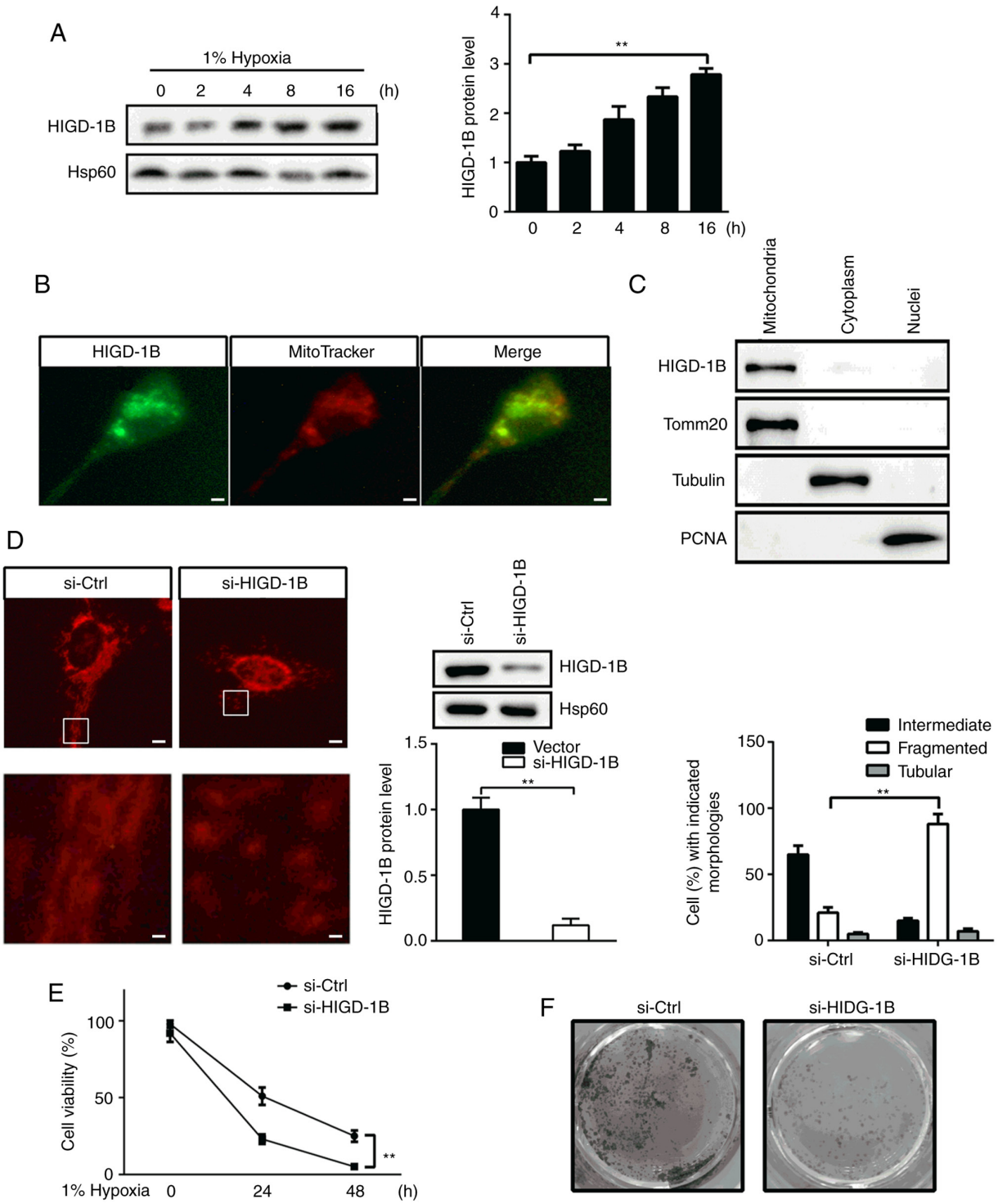

Figure 1. Knockdown of HIGD-1B induces mitochondrial fragmentation. (A) AC16 cells were cultured under hypoxic conditions, then the protein expression levels of HIGD-1B were measured using western blot analysis. (B) Representative immunofluorescence image of anti-HIGD-1B antibody (green)-stained AC16 cells. MitoTracker is a red fluorescent mitochondrial stain. Scale bar, 10 μm. (C) Western blot analysis of HIGD-1B expression levels in proteins extracted from the cytoplasm, mitochondria and nucleus of AC16 cells under normoxic conditions. (D) AC16 cells were transfected with si-Ctrl or si-HIGD-1B, then stained with MitoTracker, fixed and mounted for microscopy. The illustration is an enlarged view of the boxed area. In each group, >100 cells in five fields of view were measured to determine the percentages of the cells with tubular, intermediate and fragmented mitochondria. Scale bar, 2 μm. (E) Cell Counting Kit-8 assay was used to evaluate the viability of AC16 cells following transfection with si-Ctrl or si-HIGD-1B under hypoxic conditions. (F) AC16 cells were transfected with si-Ctrl or si-HIGD-1B, then cultured under hypoxic conditions for 48 h. The cells were visualized using crystal violet staining. The data are presented as the mean ± SEM. **P<0.01. si, small interfering; Ctrl, control; HIGD-1B, HIG1 hypoxia inducible domain family member 1B; Tomm20, translocase of outer mitochondrial membrane 20; PCNA, proliferating cell nuclear antigen.

with MitotTacker. Downregulation of *HIGD-1B* via transfection with siRNA resulted in fragmented mitochondria in 88.2±7.5% of cells (Fig. 1D). The effect of HIGD-1B on AC16 cell viability was also determined. Silencing of *HIGD-1B* resulted in decreased cell viability compared with that of control cells following hypoxia (Fig. 1E). Furthermore, crystal

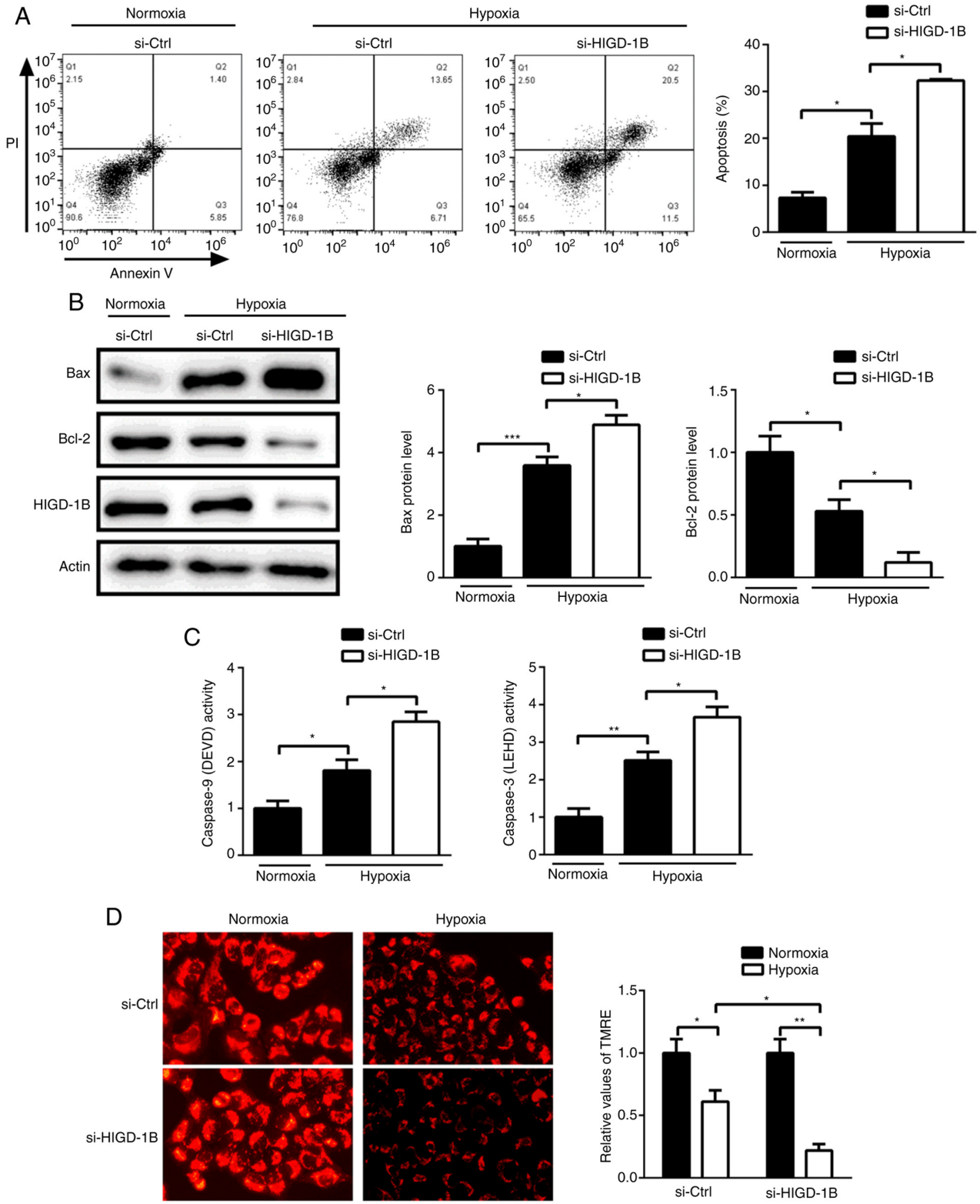

Figure 2. Knockdown of HIGD-1B promotes hypoxia-induced cell death. Following transfection with si-Ctrl or si-HIGD-1B under normoxic or hypoxic conditions, (A) Annexin V/PI staining and (B) detection of Bax, Bcl-2 and HIGD1B protein expression levels were performed, and (C) caspase-3 and -9 activity levels and (D) mitochondrial membrane potential were analyzed using flow cytometry, western blot analysis, caspase assay and tetramethylrhodamine ethyl ester perchlorate, respectively. Caspase-9 activity was measured using luminogenic substrate of DEVD and caspase-3 activity was measured using luminogenic substrate of LEHD. Data are presented as the mean ± SEM. *P<0.05, **P<0.01, ***P<0.001. si-, small interfering RNA, Ctrl, control; HIGD-1B, HIG1 hypoxia inducible domain family member 1B; DEVD, Ac-DEVD-AMC; LEHD, Z-LEHD-aminoluciferin; TMRE, tetramethylrhodamine methyl ester.

violet staining demonstrated that there were fewer viable cells observed in the si-HIGD-1B group compared with the si-Ctrl group under hypoxic conditions for 48 h (Fig. 1F). Taken together, these data suggested that HIGD-1B knockdown affected mitochondrial fusion and decreased viability in AC16 cells.

Silencing of HIGD-1B promotes hypoxia-induced apoptosis. Next, the effect of HIGD-1B on hypoxia-induced apoptosis was investigated. Annexin V/PI staining showed that knockdown of HIGD-1B promoted hypoxia-induced apoptosis (Fig. 2A). Western blot analysis showed that HIGD-1B knockdown increased the protein expression levels of Bcl-2 and decreased those of Bax under hypoxic conditions (Fig. 2B). Furthermore, HIGD-1B-knockdown cells exhibited higher caspase-3 and -9 activity compared with that control cells, suggesting that HIGD-1B regulated mitochondrial-mediated apoptosis via the caspase signaling pathway (Fig. 2C). Following hypoxia, AC16 cells exhibited decreased TMRE fluorescence compared with cells treated under normoxic conditions. Silencing of HIGD-1B further decreased the TMRE signal, indicating that HIGD-1B knockdown decreased the mitochondrial membrane potential of AC16 cells under hypoxic conditions (Fig. 2D). Taken together, these data indicated that HIGD-1B silencing promoted hypoxia-induced cell death by regulating caspase signaling in the AC16 cells.

Silencing of HIGD-1B promotes degradation of L-OPA1. The aforementioned results demonstrated that HIGD-1B was required for optimal fusion of mitochondria; therefore, the role of HIGD-1B in fusion- and fission-associated protein expression levels was investigated. Protein expression levels of OMA1, YME1L and outer mitochondrial membrane proteins MFN-1 and -2 were unchanged in HIGD-1B-knockdown cells, indicating that HIGD-1B was not responsible for outer membrane fusion (Fig. 3A). OPA1 protein is produced by eight different alternative splicing forms of mRNA, which are cleaved by proteases (12). Therefore, five different OPA1 bands (Fig. 3B) were observed using western blot analysis. Notably, knockdown of HIGD-1B resulted in a decrease in the expression levels of L-OPA1 and increase in S-OPA1, whereas HIGD-1B overexpression increased the expression levels of the larger band (Fig. 3B). In addition, activated DRP was unchanged following knockdown or overexpression of HIGD-1B (Fig. 3C). These results indicated that mitochondrial fragmentation in HIGD-1B-knockdown cells could change the isoform of OPA1.

HIGD-1B physically interacts with OPA1. In order to identify the molecular mechanism underlying the association between HIGD-1B and OPA1, it was determined whether HIGD-1B interacted with OPA1. Co-IP analysis showed that exogenous HIGD-1B interacted with OPA1 in 293T cells (Fig. 4A). In order to confirm this result, endogenous IP assay was performed. OPA1 was present in larger amounts in the immunoprecipitate with the anti-HIGD-1B antibody compared with the control IgG group (Fig. 4B). The result was confirmed using an *in vitro* pull-down assay. Myc-OPA1 was precipitated specifically by recombinant GST-HIGD-1B, but not by GST-alone (Fig. 4C). Taken together, these results demonstrated that HIGD-1B directly interacted with OPA1 and affected its cleavage.

HIGD-1B overexpression restricts the cleavage of OPA1. In order to determine the function of HIGD-1B, it was investigated whether overexpression of HIGD-1B inhibited cleavage of OPA1. Under hypoxic conditions, the L-OPA1 isoform gradually disappeared, whereas the S-OPA1 isoform accumulated. Cleavage of the L-OPA1 bands was observed in cells transfected with empty vector for 12 h, whereas overexpression of HIGD-1B delayed cleavage for up to 24 h under hypoxic conditions (Fig. 5A). Treatment of AC16 cells with CCCP also resulted in OPA1 cleavage, whereas HIGD-1B overexpression stabilized the L-OPA1 isoform for up to 15 min (Fig. 5B). This indicated that HIGD-1B delayed cleavage of OPA1 but did not restrict it completely. HIGD-1B overexpression prevented hypoxia-induced mitochondrial fragmentation (Fig. 5C). Furthermore, HIGD-1B-Flag transfected cells exhibited improved survival compared with control cells under hypoxic conditions (Fig. 5D). Similarly, the number of viable HIGD-1B-Flag transfected cells was 1-fold higher compared with control cells following CCCP treatment (10-50 μM; Fig. 5E). Based on these findings, it was concluded that HIGD-1B delayed the cleavage of OPA1 and stabilized mitochondrial morphology, thus prolonging AC16 cell survival under hypoxic conditions.

Discussion

OPA1 protein undergoes proteolytic processing, which is key for mitochondrial fusion activity, cristae organization and cell apoptosis (13,22). Cellular stress (such as hypoxia) induces mitochondrial dysfunction, which activate sOPA1 cleavage, resulting in increased conversion of L-OPA1 into S-OPA1 and mitochondrial fragmentation (22). Mitochondrial fusion is required for cardiomyocyte differentiation and cardiac development, although it occurs infrequently. The key role of OPA1 in normal cardiac function can be attributed to loss of L-OPA1 (23,24). L-OPA1 is essential for maintaining cardiac function, whereas accumulation of S-OPA1 and improper fission are deleterious for the heart. In the present study, the role of HIGD-1B in the mitochondria was identified; HIGD-1B modulated mitochondrial fusion by preventing cleavage of OPA1. Knockdown of HIGD-1B was found to enhance L-OPA1 cleavage into S-OPA1. Therefore, mitochondrial fragmentation induced by HIGD-1B knockdown may be caused by the accumulation of S-OPA1 in cardiomyocytes. Hypoxia-induced mitochondrial network changes are associated with processing of the OPA1 protein (25). For example, OPA1 is involved in hypoxia-induced cardiomyocyte death by improving mitochondrial quality control (26). Protein expression of HIGD-1B was induced by hypoxia and overexpression of HIGD-1B delayed cleavage of OPA1 induced by hypoxia or CCCP, leading to decreased mitochondrial fragmentation and increased cell viability. Accumulating evidence has revealed that different stimuli regulate OPA1 processing by YME1L or OMA1, which allows coordinated fusion and fission of mitochondria under various physiological conditions (10). Abnormal degradation of OMA1 and YME1L is involved in OPA1 dysfunction, OMA1 knockdown or YME1L overexpression can decrease TNF-α-induced cell apoptosis in H9C2 cells (27). In addition, proteases, such as presenilin-associated rhomboid-like protein mitochondrial and mitochondrial-AAA, are involved in OPA1 cleavage (28,29). Knockdown of YME1L activates OMA1, which increases conversion of L-OPA1 into S-OPA1 and mitochondrial fragmentation (12,30). Here, HIGD-1B did not affect the protein expression levels of YME1L or OMA1, suggesting that HIGD-1B did not regulate

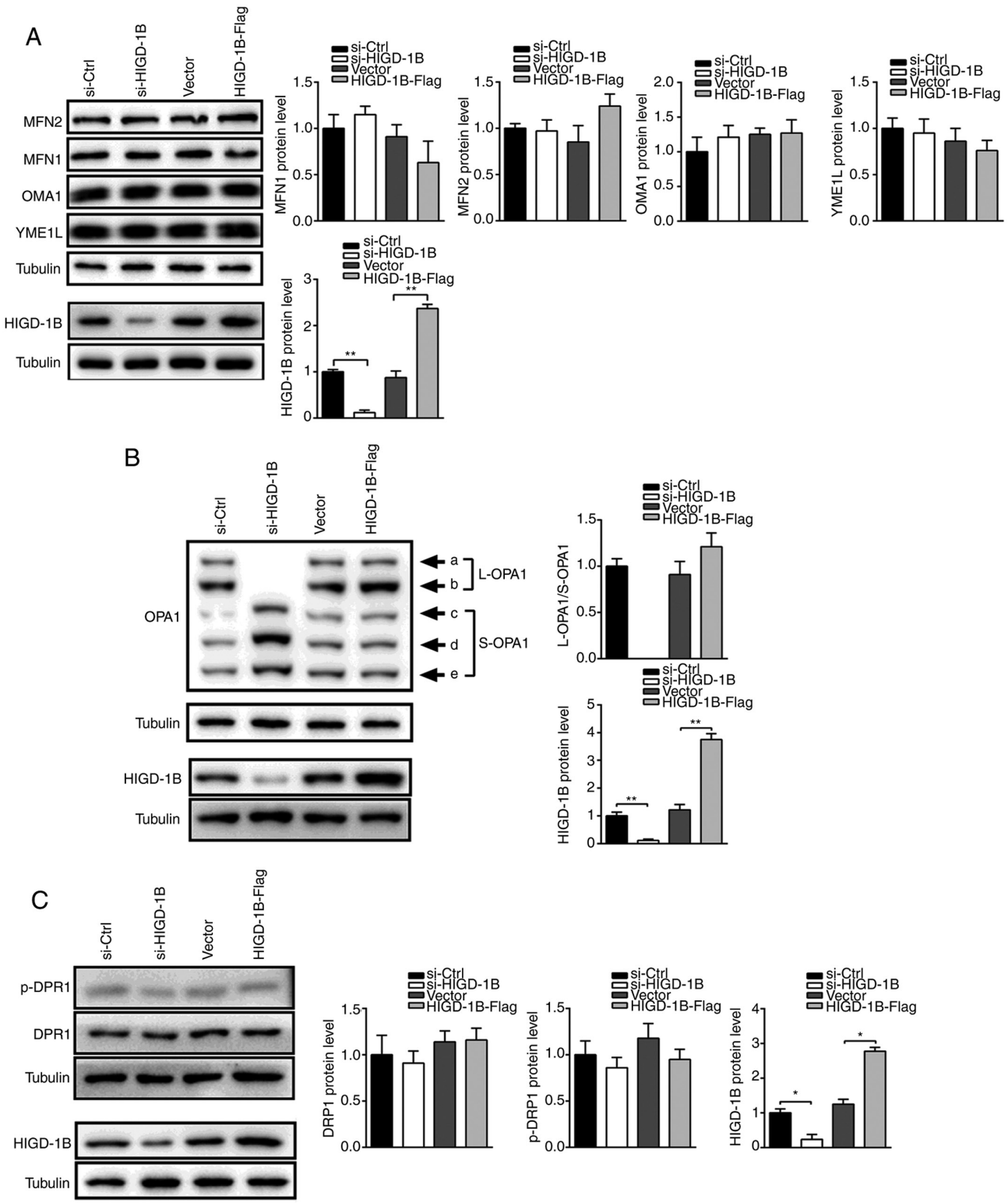

Figure 3. HIGD-1B regulates OPA1 cleavage. Western blot analysis was performed to evaluate the protein expression levels of (A) HIGD-1B, MFN1, MFN2, OMA1 and YME1L. Western blot analysis was performed to evaluate the protein expression levels of (B) OPA1 and HIGD-1B. Western blot analysis was performed to evaluate the protein expression levels of (C) DRP1, p-DRP1 and HIGD-1B following transfection. The data are presented as the mean ± SEM. *P<0.05, **P<0.01. p-, phosphorylated; HIGD-1B, HIG1 hypoxia inducible domain family member 1B; MFN, mitofusin; OMA1, metalloendopeptidase OMA1, mitochondrial; YME1L, ATP-dependent zinc metalloprotease YME1L1; OPA1, optic atrophy 1; DRP1, dynamin-related protein 1; L, long; S, short; si-, small interfering RNA; Ctrl, control.

the cleavage of OPA1 via YME1L or OMA1, but by directly interacting with OPA1. Furthermore, HIGD-1B was not responsible for outer membrane fusion as HIGD-1B did not affect the protein expression levels of the outer mitochondrial membrane proteins MFN-1 and -2. DRP1 is a mitochondrial fission protein localized in the cytosol that is recruited to mitochondria, and divides the outer and inner membranes of the mitochondrion (31). Considering that HIGD-1B did not alter the activity of DRP1, it was hypothesized that HIGD-1B is not necessary for mitochondrial fission.

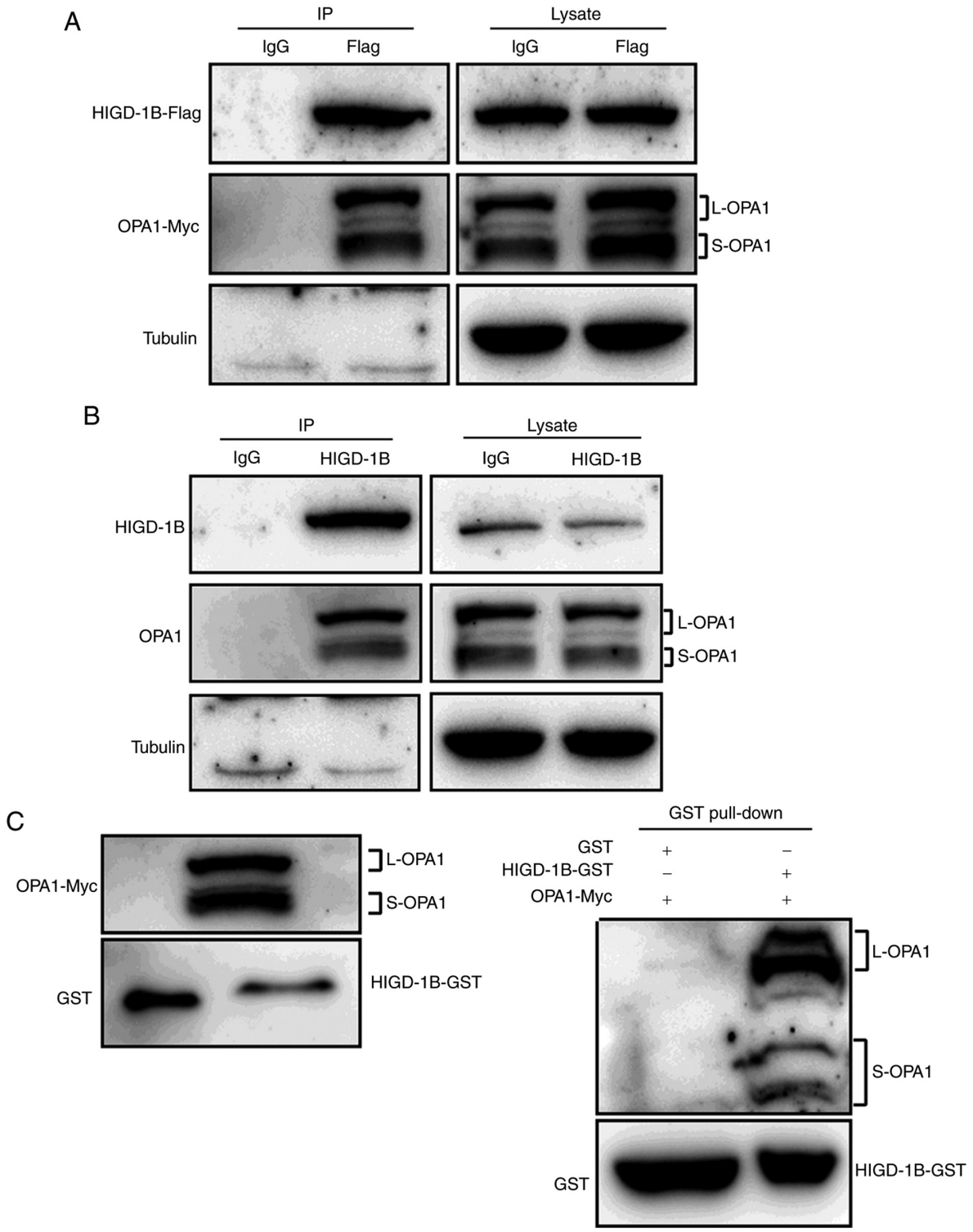

Figure 4. HIGD-1B interacts with OPA1. The 293T cells were co-transfected with plasmids. Cell lysates were immunoprecipitated with (A) anti-Flag and (B) HIGD-1B antibody or control IgG, followed by western blot analysis. (C) SDS-PAGE for the purified GST-tagged HIGD-1B, Myc-tagged and GST proteins. Purified GST-HIGD-1B or GST protein bound to glutathione-Sepharose 4B was incubated with purified Myc-OPA1. Bound complexes were analyzed via western blot analysis using anti-GST or anti-Myc. GST, glutathione S-transferase; HIGD-1B, HIG1 hypoxia inducible domain family member 1B; OPA1, optic atrophy 1; L, long; S, short.

HIGD-1A and HIGD-2A both serve an anti-apoptotic function in response to hypoxia; however, the regulatory mechanisms involved are not identical. HIGD-2A is localized to the mitochondrial network and the nucleus, whereas HIGD-1A is only co-localized with mitochondria (32). HIGD-1A silencing has been found to not alter mitochondria membrane potential or cellular ATP, whereas knockdown of HIGD-2A in 293T cells can increase the mitochondrial membrane potential (20,32). Unlike HIGD-1A, HIGD-2A is also associated with OPA1; however, decreased HIGD-2A protein expression has no effect on OPA1 cleavage (21,33). Similar to HIGD-1A, HIGD-1B is primarily expressed in the brain, heart and kidney (21). The results from the present study showed that HIGD-1B co-localized with the mitochon-

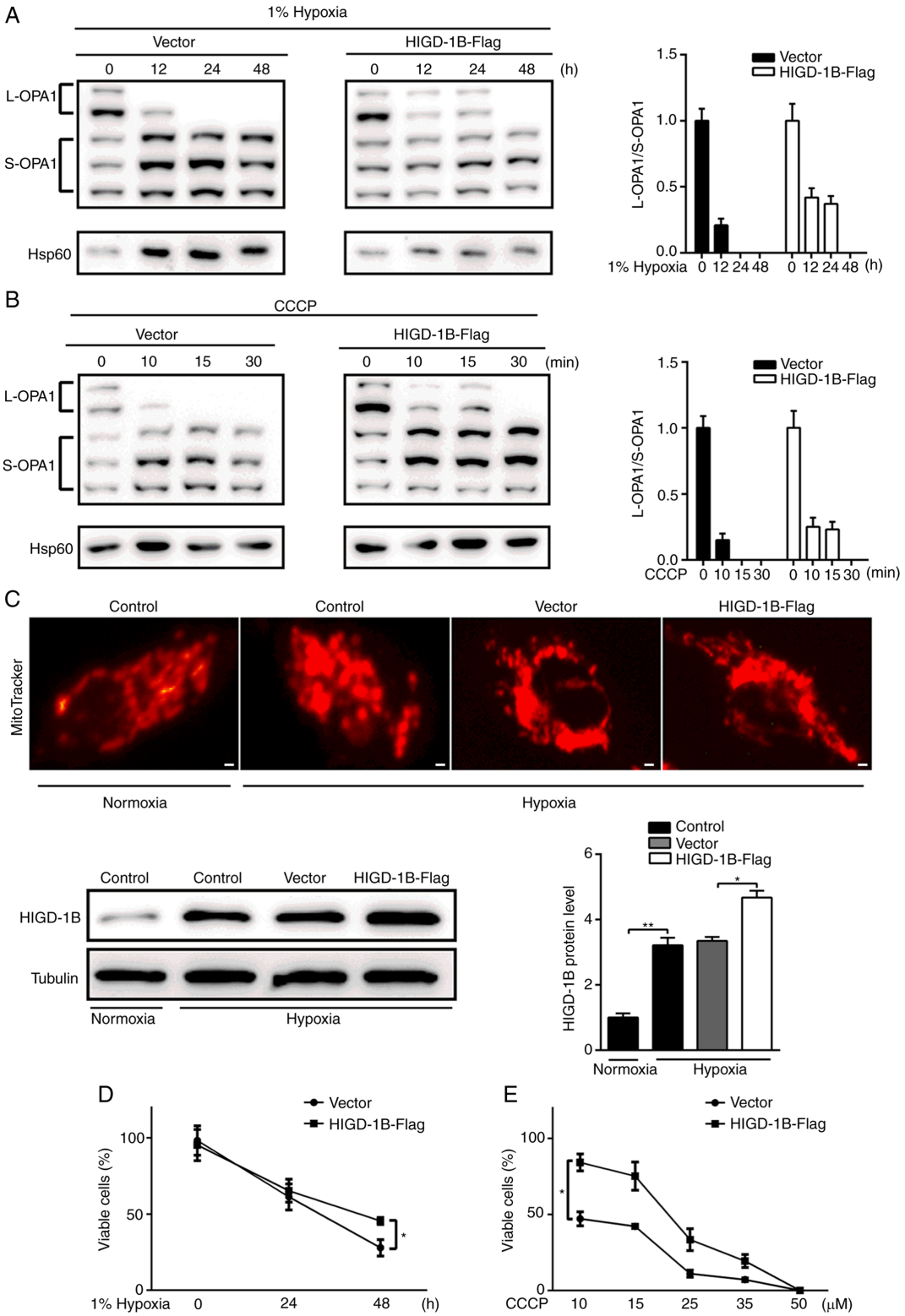

Figure 5. HIGD-1B delays OPA1 cleavage. (A) AC16 cells were transfected with empty or HIGD-1B-Flag vector, then incubated under hypoxic conditions. (B) Transfected AC16 cells were treated with CCCP. Total cell lysates were subjected to western blot analysis using an anti-OPA1 and Hsp60 antibodies. (C) AC16 cells were transfected with HIGD-1B-Flag or empty vector, then cultured under normoxic or hypoxic conditions. Western blotting was performed to detect HIGD-1B expression in each group. The cells were visualized under a fluorescent microscope following staining with MitoTracker. Scale bar, 10 μm. (D) AC16 cells were transfected with empty vector or HIGD-1B-Flag, then incubated under hypoxic conditions. (E) Transfected AC16 cells were treated with 10-50 μM CCCP for 1 h. Total viable cells were examined using trypan blue exclusion. Data are presented as the mean ± SEM. *P<0.05, **P<0.01. CCCP, carbonyl cyanide m-chlorophenyl hydrazone; HIGD-1B, HIG1 hypoxia inducible domain family member 1B; OPA1, optic atrophy 1; Hsp, heat shock protein; L, long; S, short.

dria and inhibited the cleavage of OPA1, suggesting that its regulatory mechanism of mitochondrial fusion was similar to HIGD-1A.

Bcl-2 family proteins are involved in hypoxia-induced apoptosis. A previous report showed that inhibition of Bcl-2 during hypoxia results in endothelial apoptosis, and this is associated

with the expression ratio of Bcl-2 and Bax (34). Furthermore, knockdown of Bax in mice results in lower mortality when deprived of oxygen and $Bax^{-/-}$ mice exhibit decreased apoptosis and caspase-3 activity following hypoxia-ischemia compared with wild-type mice (35,36). In the present study, HIGD-1B may have inhibited hypoxia-induced apoptosis by changing expression levels of Bcl-2 family proteins: HIGD-1B-knockdown cells exhibited significantly increased protein expression levels of Bax and decreased expression levels of Bcl-2. Furthermore, HIGD-1B-knockdown cells exhibited more caspase-3 and -9 activity. Based on these observations, it was hypothesized that HIGD-1B regulated the mitochondrial death pathway involving caspase. An *et al* (20) reported that knockdown of HIGD-1A in 293T cells does not induce apoptosis but inhibits proliferation. The results from the present study revealed that knockdown of HIGD-1B promoted apoptosis of cardiomyocytes cells under hypoxic conditions. Furthermore, HIGD-1A was required for optimal fusion of mitochondria in DRP1-silenced cells, whereas HIGD-1B silencing did not alter DRP1 expression levels. This may be due to different functions of the HIGD family in different cell lines (37). Hypoxia is one of the important hallmarks of tumor microenvironment (38). Thus, the role of HIGD family in tumor cells warrants further study. Overexpression of HIGD-1B delayed cleavage of OPA1, which contributed to inhibition of hypoxia or CCCP-induced mitochondrial fragmentation and cell death. In addition, the results from the present study demonstrated that *HIGD* family proteins may have a wide effect in protecting mitochondrial function. A previous study indicated that HIGD-1A in the mitochondria directly binds to γ-secretase components and attenuates hypoxia-induced γ-secretase activation on the mitochondrial membrane, thus mitigating hypoxia-induced mitochondrial dysfunction (32). HIGD-1A is induced by hypoxia in a HIF-1-dependent manner. Similarly, ROS accumulation in HepG2 cells promotes HIGD-1A expression levels by upregulating HIF-1α and PGC-1α expression levels under high-fat exposure (39). HIGD-1A inhibits the pERK/p27KIP1/retinoblastoma protein signaling pathway, which leads to cell cycle arrest (40). Collectively, HIGD isomers serve vital roles against cell death in response to stress. Given the important role of HIGD-1B in the cell hypoxia response and maintenance of mitochondrial integrity, understanding the protein interaction network underlying HIGD-1B expression may allow identification of which proteins participate in hypoxia-induced apoptosis and mitochondrial fragmentation.

Acknowledgements

Not applicable.

Funding

The present study was supported by the National Nature Science Foundation of China (grant nos. 81260522 and 81673891).

Availability of data and materials

The datasets used and/or analyzed during the current study are available from the corresponding author on reasonable request.

Authors' contributions

YP, ZW, JuL, MT, HL and JiL performed data analysis and interpretation and wrote the manuscript. ZZ and ZX designed the present study and performed the literature review. YP, ZW and JiL confirm the authenticity of all the raw data. All authors read and approved the final manuscript.

Ethics approval and consent to participate

Not applicable.

Patient consent for publication

Not applicable.

Competing interests

The authors declare that they have no competing interests.

References

1. Hoppins S, Lackner L and Nunnari J: The machines that divide and fuse mitochondria. Annu Rev Biochem 76: 751-780, 2007.
2. Burté F, Carelli V, Chinnery PF and Yu-Wai-Man P: Disturbed mitochondrial dynamics and neurodegenerative disorders. Nat Rev Neurol 11: 11-24, 2015.
3. Dorn GW II and Kitsis RN: The mitochondrial dynamism-mitophagy-cell death interactome: Multiple roles performed by members of a mitochondrial molecular ensemble. Circ Res 116: 167-182, 2015.
4. Bose A and Beal MF: Mitochondrial dysfunction in Parkinson's disease. J Neurochem 139 (Suppl 1): 216-231, 2016.
5. Smirnova E, Griparic L, Shurland DL and van der Bliek AM: Dynamin-related protein Drp1 is required for mitochondrial division in mammalian cells. Mol Biol Cell 12: 2245-2256, 2001.
6. Koshiba T, Detmer SA, Kaiser JT, Chen H, McCaffery JM and Chan DC: Structural basis of mitochondrial tethering by mitofusin complexes. Science 305: 858-862, 2004.
7. Cipolat S, Martins de Brito O, Dal Zilio B and Scorrano L: OPA1 requires mitofusin 1 to promote mitochondrial fusion. Proc Natl Acad Sci USA 101: 15927-15932, 2004.
8. Roy M, Reddy PH, Iijima M and Sesaki H: Mitochondrial division and fusion in metabolism. Curr Opin Cell Biol 33: 111-118, 2015.
9. Head B, Griparic L, Amiri M, Gandre-Babbe S and van der Bliek AM: Inducible proteolytic inactivation of OPA1 mediated by the OMA1 protease in mammalian cells. J Cell Biol 187: 959-966, 2009.
10. Rainbolt TK, Lebeau J, Puchades C and Wiseman RL: Reciprocal degradation of YME1L and OMA1 adapts mitochondrial proteolytic activity during stress. Cell Rep 14: 2041-2049, 2016.
11. Tondera D, Grandemange S, Jourdain A, Karbowski M, Mattenberger Y, Herzig S, Da Cruz S, Clerc P, Raschke I, Merkwirth C, *et al*: SLP-2 is required for stress-induced mitochondrial hyperfusion. EMBO J 28: 1589-1600, 2009.
12. Anand R, Wai T, Baker MJ, Kladt N, Schauss AC, Rugarli E and Langer T: The i-AAA protease YME1L and OMA1 cleave OPA1 to balance mitochondrial fusion and fission. J Cell Biol 204: 919-929, 2014.
13. Olichon A, Baricault L, Gas N, Guillou E, Valette A, Belenguer P and Lenaers G: Loss of OPA1 perturbates the mitochondrial inner membrane structure and integrity, leading to cytochrome c release and apoptosis. J Biol Chem 278: 7743-7746, 2003.
14. Semenza GL: Oxygen sensing, hypoxia-inducible factors, and disease pathophysiology. Annu Rev Pathol 9: 47-71, 2014.
15. Parra V, Bravo-Sagua R, Norambuena-Soto I, Hernández-Fuentes CP, Gómez-Contreras AG, Verdejo HE, Mellado R, Chiong M, Lavandero S and Castro PF: Inhibition of mitochondrial fission prevents hypoxia-induced metabolic shift and cellular proliferation of pulmonary arterial smooth muscle cells. Biochim Biophys Acta Mol Basis Dis 1863: 2891-2903, 2017.

16. Bedo G, Vargas M, Ferreiro MJ, Chalar C and Agrati D: Characterization of hypoxia induced gene 1: Expression during rat central nervous system maturation and evidence of antisense RNA expression. Int J Dev Biol 49: 431-436, 2005.
17. Wang J, Cao Y, Chen Y, Chen Y, Gardner P and Steiner DF: Pancreatic beta cells lack a low glucose and O_2-inducible mitochondrial protein that augments cell survival. Proc Natl Acad Sci USA 103: 10636-10641, 2006.
18. Hayashi T, Asano Y, Shintani Y, Aoyama H, Kioka H, Tsukamoto O, Hikita M, Shinzawa-Itoh K, Takafuji K, Higo S, *et al*: Higd1a is a positive regulator of cytochrome c oxidase. Proc Natl Acad Sci USA 112: 1553-1558, 2015.
19. Ameri K, Jahangiri A, Rajah AM, Tormos KV, Nagarajan R, Pekmezci M, Nguyen V, Wheeler ML, Murphy MP, Sanders TA, *et al*: HIGD1A regulates oxygen consumption, ROS production, and AMPK activity during glucose deprivation to modulate cell survival and tumor growth. Cell Rep 10: 891-899, 2015.
20. An HJ, Cho G, Lee JO, Paik SG, Kim YS and Lee H: Higd-1a interacts with Opa1 and is required for the morphological and functional integrity of mitochondria. Proc Natl Acad Sci USA 110: 13014-13019, 2013.
21. An HJ, Shin H, Jo SG, Kim YJ, Lee JO, Paik SG and Lee H: The survival effect of mitochondrial Higd-1a is associated with suppression of cytochrome C release and prevention of caspase activation. Biochim Biophys Acta 1813: 2088-2098, 2011.
22. Ishihara N, Fujita Y, Oka T and Mihara K: Regulation of mitochondrial morphology through proteolytic cleavage of OPA1. EMBO J 25: 2966-2977, 2006.
23. Chen Y, Liu Y and Dorn GW II: Mitochondrial fusion is essential for organelle function and cardiac homeostasis. Circ Res 109: 1327-1331, 2011.
24. Papanicolaou KN, Khairallah RJ, Ngoh GA, Chikando A, Luptak I, O'Shea KM, Riley DD, Lugus JJ, Colucci WS, Lederer WJ, *et al*: Mitofusin-2 maintains mitochondrial structure and contributes to stress-induced permeability transition in cardiac myocytes. Mol Cell Biol 31: 1309-1328, 2011.
25. Baburamani AA, Hurling C, Stolp H, Sobotka K, Gressens P, Hagberg H and Thornton C: Mitochondrial optic atrophy (OPA) 1 processing is altered in response to neonatal hypoxic-ischemic brain injury. Int J Mol Sci 16: 22509-22526, 2015.
26. Xin T, Lv W, Liu D, Jing Y and Hu F: Opa1 reduces hypoxia-induced cardiomyocyte death by improving mitochondrial quality control. Front Cell Dev Biol 8: 853, 2020.
27. Wu B, Li J, Ni H, Zhuang X, Qi Z, Chen Q, Wen Z, Shi H, Luo X and Jin B: TLR4 activation promotes the progression of experimental autoimmune myocarditis to dilated cardiomyopathy by inducing mitochondrial dynamic imbalance. Oxid Med Cell Longev 2018: 3181278, 2018.
28. Ehses S, Raschke I, Mancuso G, Bernacchia A, Geimer S, Tondera D, Martinou JC, Westermann B, Rugarli EI and Langer T: Regulation of OPA1 processing and mitochondrial fusion by m-AAA protease isoenzymes and OMA1. J Cell Biol 187: 1023-1036, 2009.
29. Cipolat S, Rudka T, Hartmann D, Costa V, Serneels L, Craessaerts K, Metzger K, Frezza C, Annaert W, D'Adamio L, *et al*: Mitochondrial rhomboid PARL regulates cytochrome c release during apoptosis via OPA1-dependent cristae remodeling. Cell 126: 163-175, 2006.
30. Zhang K, Li H and Song Z: Membrane depolarization activates the mitochondrial protease OMA1 by stimulating self-cleavage. EMBO Rep 15: 576-585, 2014.
31. Mears JA, Lackner LL, Fang S, Ingerman E, Nunnari J and Hinshaw JE: Conformational changes in Dnm1 support a contractile mechanism for mitochondrial fission. Nat Struct Mol Biol 18: 20-26, 2011.
32. Hayashi H, Nakagami H, Takeichi M, Shimamura M, Koibuchi N, Oiki E, Sato N, Koriyama H, Mori M, Gerardo Araujo R, *et al*: HIG1, a novel regulator of mitochondrial γ-secretase, maintains normal mitochondrial function. FASEB J 26: 2306-2317, 2012.
33. Salazar C, Elorza AA, Cofre G, Ruiz-Hincapie P, Shirihai O and Ruiz LM: The OXPHOS supercomplex assembly factor HIG2A responds to changes in energetic metabolism and cell cycle. J Cell Physiol 234: 17405-17419, 2019.
34. Matsushita H, Morishita R, Nata T, Aoki M, Nakagami H, Taniyama Y, Yamamoto K, Higaki J, Yasufumi K and Ogihara T: Hypoxia-induced endothelial apoptosis through nuclear factor-kappaB (NF-kappaB)-mediated bcl-2 suppression: In vivo evidence of the importance of NF-kappaB in endothelial cell regulation. Circ Res 86: 974-981, 2000.
35. McClintock DS, Santore MT, Lee VY, Brunelle J, Budinger GR, Zong WX, Thompson CB, Hay N and Chandel NS: Bcl-2 family members and functional electron transport chain regulate oxygen deprivation-induced cell death. Mol Cell Biol 22: 94-104, 2002.
36. Gibson ME, Han BH, Choi J, Knudson CM, Korsmeyer SJ, Parsadanian M and Holtzman DM: BAX contributes to apoptotic-like death following neonatal hypoxia-ischemia: Evidence for distinct apoptosis pathways. Mol Med 7: 644-655, 2001.
37. Timón-Gómez A, Bartley-Dier EL, Fontanesi F and Barrientos A: HIGD-driven regulation of cytochrome c oxidase biogenesis and function. Cells 9: 9, 2020.
38. Francis A, Venkatesh GH, Zaarour RF, Zeinelabdin NA, Nawafleh HH, Prasad P, Buart S, Terry S and Chouaib S: Tumor hypoxia: A key determinant of microenvironment hostility and a major checkpoint during the antitumor response. Crit Rev Immunol 38: 505-524, 2018.
39. Li T, Xian WJ, Gao Y, Jiang S, Yu QH, Zheng QC and Zhang Y: Higd1a protects cells from lipotoxicity under High-Fat Exposure. Oxid Med Cell Longev 2019: 6051262, 2019.
40. An HJ, Ryu M, Jeong HJ, Kang M, Jeon HM, Lee JO, Kim YS and Lee H: Higd-1a regulates the proliferation of pancreatic cancer cells through a pERK/p27KIP1/pRB pathway. Cancer Lett 461: 78-89, 2019.